JACS
JOURNAL OF THE AMERICAN CHEMICAL SOCIETY

Article

Selective Catalytic Reduction over Cu/SSZ-13: Linking Homo- and Heterogeneous Catalysis

Feng Gao, Donghai Mei, Yilin Wang, János Szanyi, and Charles H. F. Peden

J. Am. Chem. Soc., **Just Accepted Manuscript** • DOI: 10.1021/jacs.7b01128 • Publication Date (Web): 13 Mar 2017

Selective Catalytic Reduction over Cu/SSZ-13: Linking Homo- and Heterogeneous Catalysis

Feng Gao*, Donghai Mei*, Yilin Wang, János Szanyi, Charles H. F. Peden

Institute for Integrated Catalysis, Pacific Northwest National Laboratory, P.O. Box 999, Richland, WA 99352 (USA)

KEYWORDS: Heterogeneous catalysis • homogeneous catalysis • selective catalytic reduction • zeolite • exhaust emission

ABSTRACT: Active centers in Cu/SSZ-13 selective catalytic reduction (SCR) catalysts have been recently identified as isolated Cu^{2+} and $[Cu^{II}(OH)]^+$ ions. A redox reaction mechanism has also been established, where Cu-ions cycle between Cu^I and Cu^{II} oxidation states during SCR reaction. While the mechanism for the reduction half-cycle ($Cu^{II} \rightarrow Cu^I$) is reasonably well understood, that for the oxidation half-cycle ($Cu^I \rightarrow Cu^{II}$) remains an unsettled debate. Herein we report detailed reaction kinetics on low-temperature standard NH_3-SCR, supplemented by DFT calculations, as strong evidence that the low-temperature oxidation half-cycle occurs with the participation of two isolated Cu^I ions, via formation of a transient $[Cu^I(NH_3)_2]^+$-O_2-$[Cu^I(NH_3)_2]^+$ intermediate. The feasibility of this reaction mechanism is confirmed from DFT calculations, and the simulated energy barrier and rate constants are consistent with experimental findings. Significantly, the low-temperature standard SCR mechanism proposed here provides full consistency with low-temperature SCR kinetics.

INTRODUCTION

Cu-exchanged SSZ-13 has recently been commercialized as a selective catalytic reduction (SCR) catalyst for diesel engine exhaust aftertreatment[1-3]. This is a significant achievement in environmental catalysis, in some sense comparable to the commercialization of three-way catalysts for the cleaning of gasoline engine exhausts in the 1970s. Cu/SSZ-13 is also structurally one of the simplest Cu/zeolites for fundamental SCR investigations. Experimental and theoretical studies using this catalyst, even though only initiated less than a decade ago, have already greatly expanded our understanding of the SCR chemistry[1, 4-9]. Most significant recent mechanistic proposals for standard ammonia SCR ($4NO + 4NH_3 + O_2 = 4N_2 + 6H_2O$), derived from these studies, include: (1) isolated copper ions (Cu^{2+} and $[Cu^{II}(OH)]^+$) act as active centers; and (2) SCR follows a redox reaction mechanism – that is, copper ions cycle between +2 and +1 oxidation states during catalysis. The latter has received rather strong experimental support from in situ XAS and XES investigations[9-11]: under low-temperature standard SCR conditions, the coexistence and interconversion of Cu(II) and Cu(I) moieties has been repeatedly confirmed. The former proposal is more difficult to confirm via spectroscopic means alone, but appears more suitable to elucidate from reaction kinetics. For example, by conducting reaction under kinetic control on catalysts with varying concentrations of isolated Cu-ions, in principle one can readily judge whether SCR is independently catalyzed by isolated Cu-ions by normalizing reaction rates on a per Cu-ion basis. By doing so, however, we discovered complex Cu loading and reaction temperature dependent kinetic behavior for this reaction.[5]

In this paper, we aim to unravel this complexity by proposing that, depending on reaction conditions (especially reaction temperature), Cu-ions act either homogeneously or heterogeneously during ammonia SCR, delivering the same overall chemistry via significantly different mechanisms. In the low-temperature regime (i.e., ~150-250 °C), Cu-ions are solvated by NH_3, and zeolite cages are essentially filled with H_2O. Under such conditions, even though Cu/SSZ-13 is still considered as a heterogeneous catalyst, a quasi-homogeneous reaction environment exists for the active Cu-ion centers.[5] We further demonstrate that redox cycling cannot be achieved by isolated, individual Cu-ions in this temperature regime. Instead, key intermediates form via participation of two isolated Cu-ions acting in consort. Only at reaction temperatures above ~300 °C do Cu-ions lose NH_3 solvation and anchor at zeolite framework windows, where they act as heterogeneous, individual active sites. These two kinetic regimes naturally link homo- and heterogeneous catalysis, show-

casing the complex influences from the reaction media on the dynamics of the active sites, and further to the kinetics of the targeted chemistry.

RESULTS AND DISCUSSION

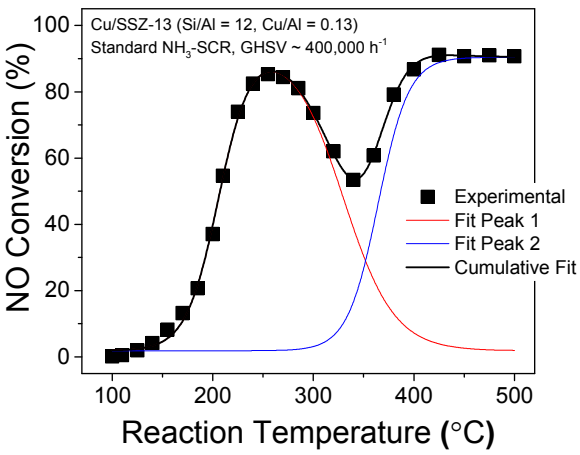

Figure 1. NO conversion versus temperature data (■) in standard SCR over a Cu/SSZ-13 catalyst with Si/Al = 12 and Cu/Al = 0.13. Reactant feed contains 350 ppm NO, 14% O_2, 2.5% H_2O balanced with N_2 at a gas hourly space velocity (GHSV) of 400,000 h^{-1}. Also included are simulated curves assuming low- and high-temperature reaction routes.

SCR Kinetics. Figure 1 displays a light-off curve for NO conversions during standard NH_3-SCR for a model Cu/SSZ-13 catalyst with Si/Al = 12 and Cu/Al = 0.13. An interesting feature of this light-off curve is that, from ~250 to ~350 °C, NO conversions actually *decrease* with increasing temperature. This phenomenon is highly unusual, and cannot be explained from common considerations such as thermodynamic limitations, or catalyst poisoning. Note that this phenomenon is highly reproducible, occurs for low to intermediate Cu-loaded Cu/SSZ-13 catalysts with various Si/Al ratios, as well as from differential to much higher conversions.[5] This interesting kinetic behavior, however, is omitted by most researchers due, primarily, to the fact that achieving high NOx conversions has always been a focus for practical SCR studies and, as such, SCR reaction measurements are typically carried out at low to moderate space velocities and on catalysts with high Cu loadings. Under such conditions, NOx conversions are typically higher than 90% in the temperature window where the abnormal "dip" in reactivity is observed. A straightforward hypothesis can be proposed to explain this unusual kinetic behavior, as indicated by peak fitting of the experimental data: there exist two reaction routes, a low-temperature route that peaks at ~250 °C and declines at higher temperatures; and a high-temperature route that "lights off" above 350 °C.

It has been recognized for some time that Cu-ions in Cu/SSZ-13 are mobile under certain circumstances; for example, they move closer to the CHA windows during dehydration, and move away from these positions upon interaction with probe molecules (e.g., CO).[12, 13] To reveal whether temperature induced changes in active site positioning can account for the unusual kinetic behavior shown in Figure 1, a series of model Cu/SSZ-13 catalysts (Si/Al = 6, 0.006 ≤ Cu/Al ≤ 0.45) were used to study Cu loading dependence on SCR kinetics. Specifically, in order for kinetic data to be collected under strict differential conditions at both low and high reaction temperatures, model catalysts with very low Cu loadings (Cu/Al ≤ 0.05) were used. For these model catalysts, electron paramagnetic resonance (EPR) and temperature-programmed reduction (TPR) analyses indicate that Cu-ions in these samples are indistinguishable under the conditions where these measurements were conducted.[5] If one assumes that reaction measurements are conducted under kinetic limitation, then it follows that turnover frequencies (e.g., normalized reaction rates on a per Cu-atom basis) should not vary for these samples, as long as catalytic turnover takes place on isolated Cu-ions *independently*, as hypothesized in a few recent SCR mechanistic studies.[7-9]

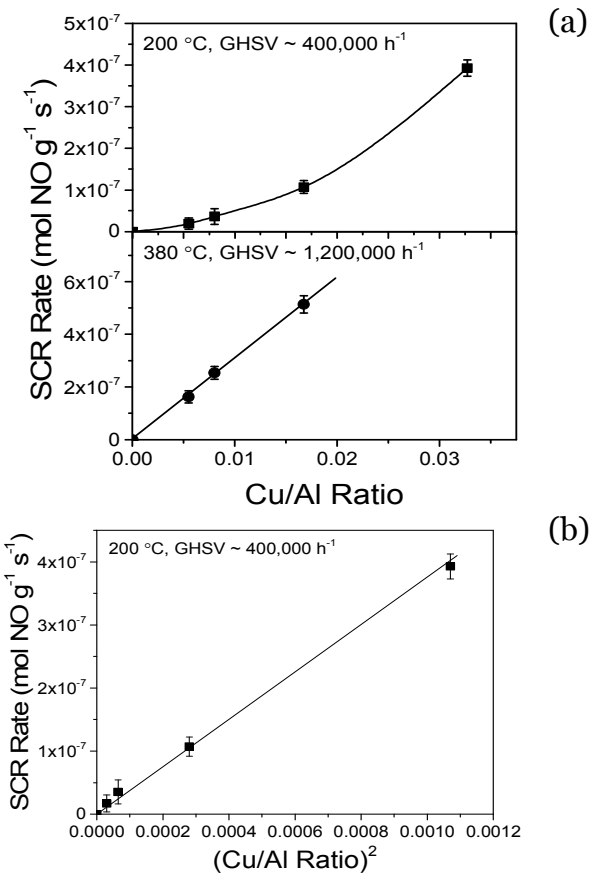

Figure 2. (a) SCR rate versus Cu/Al ratio results obtained at two reaction temperatures: 200 °C (upper panel) and 380°C (lower panel). All data points were acquired under differential reaction conditions on low Cu-loaded samples (Cu/Al < 0.05). (b) SCR rate versus $(\text{Cu/Al ratio})^2$, replotted using data shown in the upper panel of (a). Error bars represent standard errors of three measurements.

Yet, this hypothesis is only proven to be rigorously correct at temperatures above ~350 °C, but is apparently not the case at lower reaction temperatures.[5] Figure 2(a) presents correlations between normalized SCR rates (mol

NO g^{-1} s^{-1}) as a function of Cu/Al ratios (i.e., Cu content) at two reaction temperatures: 200 and 380 °C. SCR rates increase linearly with Cu/Al ratios at 380 °C (lower panel). This indicates that the Koros-Nowak criterion[5, 6] is fully obeyed, i.e., SCR reaction is carried out in the absence of mass and heat transfer limitations. Furthermore, the invariant turnover frequencies (i.e., rate normalized on a per Cu-atom basis) strongly suggests that SCR is indeed carried out on isolated Cu-ions, and that each isolated Cu-ion catalyzes SCR independently. However at 200 °C (upper panel), SCR rates increase much faster with increasing Cu/Al ratios than that expected from a linear dependence. More significantly, as displayed in Figure 2(b), SCR rates increase linearly with the *square of Cu/Al ratio*, suggesting the participation of two isolated Cu-ions in rate-limiting step(s). Note that such linear correlations with $(\text{Cu/Al ratios})^2$ are observed up to ~250°C, as long as kinetic measurements are carefully performed under differential conditions. To rationalize this kinetic behavior, we previously suggested that, at low Cu loadings, low-temperature SCR is catalyzed by "transient Cu-dimers".[5] This notion needs better clarification, which will be presented in the following. Note also that the Koros-Nowak criterion is not fully obeyed on the low Cu-loaded catalysts at such low temperatures.[5] Explanations will be given below in terms of transport limitations from the migration of active sites (rather than reactants).

Kinetic data shown in Figure 2(b) is most reasonably rationalized by invoking the participation of two isolated Cu-ions in rate-limiting step(s). This indicates that, in highly dilute catalysts, extensive migration of isolated Cu-ions between SSZ-13 unit cells has to occur. Macroscopic Cu-ion mobility has recently been recognized under typical SCR reaction conditions. For example, by exposing a Cu_2O + H/SSZ-13 physical mixture to SCR reactants at 250 °C, isolated Cu-ions readily migrate into the bulk of the zeolite crystals.[14] In a very recent operando XAS/XES study by Lomachenko et al., mobile Cu(II) and Cu(I) sites, solvated by NH_3, were identified as the primary Cu sites at 150 °C,[11] consistent with theoretical calculations by Paolucci, et al.[9] It appears, however, that a linear $[Cu^I(NH_3)_2]^+$ species is the most likely Cu-containing moiety that transports between unit cells with readily manageable energy barriers.[9, 15]

To better understand the unusual Cu-loading dependent kinetics discovered at low reaction temperatures, kinetic measurements were extended to samples with a broader range of Cu loadings. In this case, the Arrhenius equation $k = \frac{r}{[NO]_0} = Ae^{-\frac{E_a}{RT}}$ was used for detailed kinetics analysis, where k is the rate constant, r is the normalized SCR rate (mol NO g^{-1} s^{-1}), and $[NO]_o$ is the molar inlet NO concentration.[16] Using differential kinetic data collected below ~200 °C, preexponential factors, A, and apparent activation energies, E_a, were obtained and plotted in Figure 3 as a function of Cu loading, where Cu loading is now displayed as numbers of Cu ions in each hexagonal unit cell of SSZ-13 (36 T and 72 O atoms). Here, a Cu-loading dependence is again clearly demonstrated: in exceedingly dilute catalysts (< 0.1 Cu-ion per unit cell), low E_a (~40 kJ/mol) and very small A (< 10 s^{-1}) values are obtained. In highly loaded catalysts (~1-2 Cu-ions per unit cell), a high E_a of ~80 kJ/mol and much higher A values (~10^7-10^8 s^{-1}) are obtained. At intermediate Cu loadings, A and E_a values fall in between the two limiting cases.

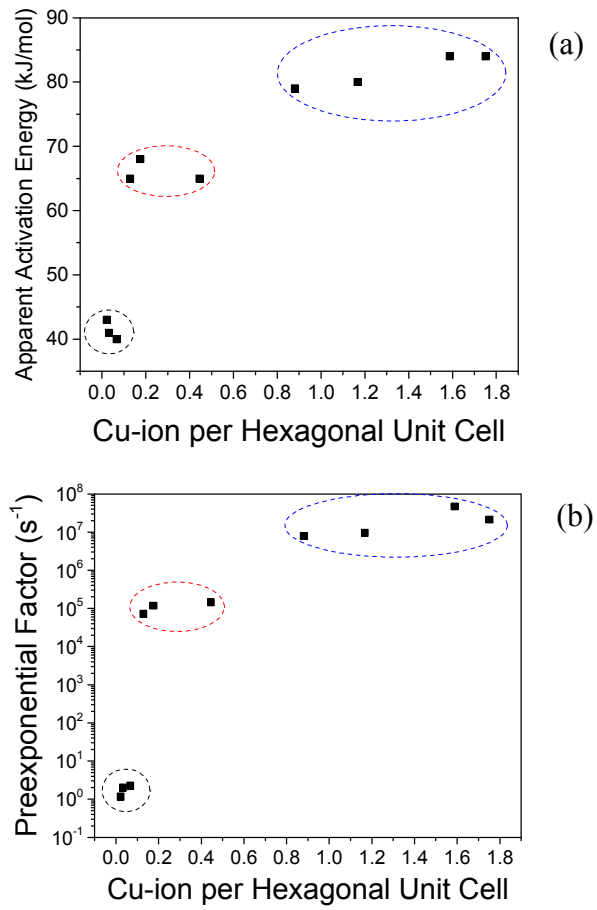

Figure 3: (a) Measured standard SCR apparent activation energy as a function of Cu loadings (Cu-ion per hexagonal unit cell of SSZ-13); (b) Measured standard SCR preexponential factors as a function of Cu loadings (Cu-ion per hexagonal unit cell of SSZ-13). Both parameters were obtained using Arrhenius equation analysis. SCR reaction was conducted at a GHSV of 400,000 h^{-1}.

A few standard SCR mechanism proposals have appeared in recent literature, derived from combined experimental and theoretical work.[2, 7-9, 17] All of these assume redox mechanisms, and share common features for the reduction half-cycle (i.e., Cu(II) → Cu(I)), but differ significantly in the oxidation half-cycle (i.e., Cu(I) → Cu(II)).[7-9] In the studies by Paolucci et al., detailed elementary steps of the oxidation half-cycle were not clearly specified,[7, 9] even though the authors indeed mentioned the possibility that a dimeric Cu species might be necessary for this half-cycle. In the work by Janssens et al., it was proposed that this chemistry is achieved via nitrate formation on single Cu(I) sites.[8] However at relatively low

temperatures the reactivity of nitrate may be questionable. Significantly, proposals that assume redox cycling of *individual isolated Cu-ions* do not account for the experimental observations obtained at low-temperature SCR conditions reported here (Figure 2). Instead, we propose that the low-temperature oxidation half-cycle of standard NH_3-SCR at low temperature only occurs with the participation of two $[Cu^I(NH_3)_2]^+$ centers. We further suggest that this is realized via formation of a transient $[Cu^I(NH_3)_2]^+$-O_2-$[Cu^I(NH_3)_2]^+$ intermediate whose formation at low Cu loadings, is the rate-limiting step. Thus, this mechanism clearly provides a satisfactory explanation for the linear rate versus square of Cu loading relationship shown in Figure 2(b).

Formation of this intermediate, i.e., the fixation of two mobile $[Cu^I(NH_3)_2]^+$ species and one gas-phase O_2 molecule, must be accompanied with an entropy loss (i.e., $\Delta S < 0$): the lower the Cu loading, the higher the entropy penalty is expected. It is further inferred from transition state theory (i.e., $k \propto e^{\frac{\Delta S^{\ddagger}}{R}} e^{-\frac{\Delta H^{\ddagger}}{RT}}$) that, if one assumes that the enthalpy change remains constant with Cu loading for the formation of this intermediate, then reaction rate constants will be primarily determined by the entropy term, which should increase with increasing Cu loading. This notion is fully consistent with Figure 3(b) where prefactors of the Arrhenius equation increase dramatically with increasing Cu loading until Cu loading reaches ~1 Cu per unit cell; above this Cu loading, it appears, understandably, that entropy variation for the formation of this intermediate become insensitive to Cu loading.

Apparent activation energy variations shown in Figure 3(a) can be explained similarly: at low Cu loadings, adsorption/desorption of the migrating $[Cu^I(NH_3)_2]^+$ centers to/from the zeolite framework appears to significantly alter the measured apparent activation energies. Note that this situation is similar to what is typically seen in mass-transfer limited reaction kinetics. In the latter case, apparent activation energies can drop to ~50% of their limitation-free values.[18] Interestingly, as shown in Figure 3(a), apparent activation energies measured at exceedingly low Cu loadings are indeed ~50% of those measured at high loadings. Therefore, even though formation of the $[Cu^I(NH_3)_2]^+$-O_2-$[Cu^I(NH_3)_2]^+$ intermediates is considered as the rate-limiting step for SCR at low Cu loadings, the ultimate limiting factor is transport of $[Cu^I(NH_3)_2]^+$ in the reaction media. Additional evidence for the presence of this special (active center) mass transfer limitation has been provided recently in studies that introduced alkali cocations to low-Cu loaded Cu/SSZ-13 catalysts. In this case, via the added K^+ and Cs^+ cations, both SCR rates and measured apparent activation energies decrease substantially in comparison to those measured on catalysts with Li^+ and Na^+ cocations.[19] A likely explanation is that K^+ and Cs^+ cations anchor preferentially to 8-membered ring openings of Chabazite,[20] thus introducing extra barriers to Cu-ion migration.

It is interesting to note that, as Cu loading increases to intermediate and high exchange levels, the linear rate versus square of Cu loading relationship, as shown in Figure 2(b), is no longer observed,[5] suggesting that formation of the $[Cu^I(NH_3)_2]^+$-O_2-$[Cu^I(NH_3)_2]^+$ intermediate is no longer the rate-limiting step. It is important to emphasize that the low-temperature oxidation half-cycle should still take place through this intermediate at moderate to high Cu loadings. This follows since, at low Cu loadings, $[Cu^I(NH_3)_2]^+$ centers choose to pay a huge entropy penalty to form the $[Cu^I(NH_3)_2]^+$-O_2-$[Cu^I(NH_3)_2]^+$ intermediate in order for Cu(I) to be reoxidized; thus, there seems no reason why the same pathway would not be adopted at high Cu loadings where the formation of this intermediate is significantly more facile.

NO light-off curve displayed in Figure 1 can now be satisfactorily explained. As reaction temperature rises above ~250°C, Cu-NH_3 complexes, that are otherwise stable at lower temperatures, dissociate. In this case, Cu-ions will migrate toward the zeolite framework ion-exchange sites, and become stabilized (also immobilized) by coordinating with the lattice oxygens. In other words, the low-temperature oxidation half-cycle is no longer possible via formation of intermediates that contain two isolated Cu-ions. In this case, the oxidation half-cycle will have to be carried out by single isolated Cu-ions as clearly demonstrated by reaction data shown in Figure 2 (lower panel). In particular, SCR rates for the *same* catalyst go from being dependent on (Cu/Al ratios)^2 to linearly dependent on Cu/Al ratios as the reaction temperature changes from 200 to 380 °C. It can be anticipated that this reoxidation process is energetically more demanding than a dual Cu-ion mechanism discussed above since, indeed, reoxidation of Cu(I) by isolated Cu ions is *not* chosen by the Cu/SSZ-13 catalyst at lower reaction temperatures. Above ~350°C, a measured apparent activation energy of ~140 kJ/mol was found for standard SCR,[5] in line with the argument that an oxidation half-cycle on isolated Cu(I)-ions is rather demanding. The SCR mechanism proposed by Janssens et al.[8], i.e., Cu(I) reoxidation is achieved by interaction with NO and O_2 to form a Cu(II)-nitrate intermediate, may be considered a successful model for high-temperature SCR catalyzed by individual Cu-ions. Indeed, the activation energy these authors calculated, i.e., ~104 kJ/mol,[8] is reasonably close to our experimental data. Spectroscopically, a temperature-induced transition from mobile to immobile states for Cu(I)/Cu(II) ions has recently been demonstrated via operando XAS/SES: while mobile NH_3-solvated Cu-ions dominate at low temperature, by 400°C their presence becomes negligible.[11]

DFT Calculations. In the following we use DFT calculations to further corroborate our experimental findings by providing simulated energetics and kinetics data of a complete redox cycle for low-temperature standard SCR that involves dual isolated Cu-ion centers in the oxidation half-cycle; the SCR mechanism thus generated is displayed in Figure 4. More details regarding these calculations are shown in the Supporting Information. We use a $[Cu^{II}(OH)]^+$ active species instead of a Cu^{2+} ion for the demonstration based on the following considerations: (1) both Cu^{2+} and $[Cu^{II}(OH)]^+$ are active centers for SCR,[9] the

latter can be readily generated by hydrolysis of the former – i.e., $Cu^{2+} + H_2O \rightleftharpoons [Cu^{II}(OH)]^+ + H^+$; (2) low-temperature SCR is catalyzed by mobile active sites; $[Cu^{II}(OH)]^+$ has a higher mobility than Cu^{2+} and particular stability within CHA cages, places where SCR is expected to occur;[21] (3) $[Cu^{II}(OH)]^+$ is energetically more favorable than Cu^{2+} in the reduction half-cycle, due mainly to H_2O formation.[9]

In our calculations, two hexagonal unit cells (72 T atoms) were used to construct the CHA structure, and a technically relevant Si/Al ratio of 11 was chosen. To start with, $[Cu^{II}(OH)]^+$ in an eight-membered ring window of

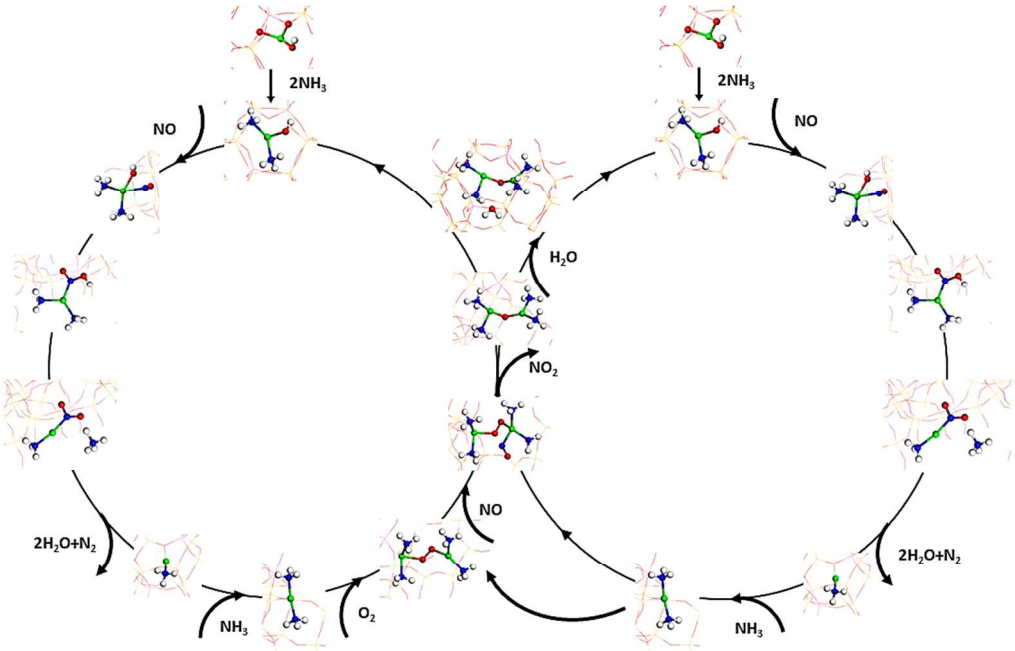

Figure 4. The complete redox cycling of low-temperature NH3-SCR derived from DFT calculations that involves two Cu(I) centers in the oxidation half-cycle.

Cu/SSZ-13 is optimized as the initial configuration of the active center in the presence of H_2O. Upon adsorption of two NH_3 molecules at the $[Cu^{II}(OH)]^+$ center, the as-formed $[(NH_3)_2\text{-}Cu^{II}\text{-}OH]^+$ intermediate detaches from the zeolite framework as a mobile complex and moves inside the CHA cage. Note that, in the recently published study by Paolucci et al, a $[(NH_3)_3\text{-}Cu^{II}\text{-}OH]^+$ intermediate has been suggested.[9] However, NO chemisorption onto this fully coordinated species would be more difficult. We note that the exact coordination numbers for NH_3 ligands may be less critical than the fact that ligating with NH_3 allows for detachment of $[Cu^{II}(OH)]^+$ from the CHA framework and, in the presence of H_2O, a quasi-homogenous reactive environment is created. Next, an NO molecule is introduced, which strongly adsorbs at the Cu^{II} center of this mobile species. Upon formation of this intermediate, NH_3 and NO ligands will rearrange, via a few energetically relatively facile elementary steps, to realize N-N bond formation. Formation of nitrosoamide (NH_2NO) or ammonium nitrite (NH_4NO_2) intermediates are frequently suggested.[22, 23] For example, Paolucci et al. suggested -NH_2NO formation in their reduction half-cycle.[7, 9] In the presence of a hydroxyl (–OH) ligand, the formation of H_2O makes formation of this intermediate energetically highly favorable.[9] On the other hand, HONO formation via interaction between –OH and NO, followed by NH_4NO_2 formation from HONO interacting with NH_3, should also be considered as a possible pathway since NH_4NO_2 is known to be highly unstable and decomposes to N_2 and H_2O readily under low-temperature SCR conditions.[23] In the present study, reduction half-cycle pathways involving both $NH_2\text{-}Cu^{I}\text{-}NO$ and $NH_3\text{-}Cu^{I}\text{-}HONO$ intermediates are calculated. Details on the energetics for the reduction half-cycle are shown in Figure S2. It appears that the "nitrite" pathway is energetically more favorable, and accordingly, this is adopted as part of the redox cycling in Figure 4. For both reduction half-cycle pathways, with N_2/H_2O formation and adsorption of another NH_3 molecule onto the copper center, the reduction half-cycle is completed, resulting in the reformation of $[Cu^{I}(NH_3)_2]^+$ as the key and most abundant intermediate in SCR mechanism, consistent with recent studies.[9, 11]

Next, we show how the oxidation half-cycle is achieved with participation of two $[Cu^{I}(NH_3)_2]^+$ intermediates, requiring that, in essence, one $[Cu^{I}(NH_3)_2]^+$ must migrate to the vicinity of another. As shown above, mobility of this linear species is key for this chemistry to be realized. The two $[Cu^{I}(NH_3)_2]^+$ intermediates and an oxygen molecule then combine to form $[Cu^{I}(NH_3)_2]^+\text{-}O_2\text{-}[Cu^{I}(NH_3)_2]^+$; subsequently electron transfer from Cu to O results in Cu-ion oxidation. However, participation of one O_2 molecule (with eventual formation of $2O^{2-}$ ions) is a four-electron reduction while oxidation of two Cu(I) centers to Cu(II) is only a two-electron process. Therefore, this chemistry is only realized in the presence of another electron provider, in this case NO, which is oxidized to NO_2. Finally, the as-formed $[Cu^{II}(NH_3)_2]^{2+}\text{-O-}[Cu^{II}(NH_3)_2]^{2+}$ intermediate is hydrolyzed by a neighboring H_2O molecule forming two $[(NH_3)_2\text{-}Cu^{II}\text{-}OH]^+$ active centers, thus closing the entire

redox cycle. Note that the generated NO_2 molecule from the oxidation half-cycle further participates in the so-called fast SCR reaction ($NO + NO_2 + 2NH_3 = 2N_2 + H_2O$). The fast SCR reaction, as its name indicates, occurs in a facile manner under typically standard SCR conditions.[1, 23] Therefore, this reaction is not further discussed here. Details regarding individual steps of the oxidation half-cycles of the standard SCR reaction are shown in Figures S3 and S4. It is important to emphasize that all of these reaction steps occur inside Cu/SSZ-13 cages in a homogeneous manner.

On the basis of our experimental kinetics shown in Figure 3, we propose a Cu-loading dependent transition in the rate-limiting step of the proposed lower (≤ 250 °C) temperature SCR mechanism. At low Cu loading conditions, formation of the $[Cu^I(NH_3)_2]^+$-O_2-$[Cu^I(NH_3)_2]^+$ intermediate (ultimately governed by transport of $[Cu^I(NH_3)_2]^+$ ions) is the rate-limiting step while, at high Cu loadings, the reaction step involving the formation of both the $[Cu^{II}(NH_3)_2]^{2+}$-O-$[Cu^{II}(NH_3)_2]^{2+}$ intermediate and NO_2 becomes rate-limiting. Using our structural model that contains two hexagonal unit cells and two isolated Cu-ion centers, the Arrhenius activation barrier and prefactor for the rate-limiting oxidation step are calculated. The obtained values, 76 kJ/mol and 9.9×10^9 s^{-1}, are consistent with our experimental values of ~80 kJ/mol and ~10^7-10^8 s^{-1} obtained at high Cu loadings (Figure 3). The calculated Gibbs free energy change of –152 kJ/mol strongly suggests that this step is thermodynamically favorable and kinetically feasible at low temperatures (e.g., 200°C). On the other hand, the relative ease of formation of the $[Cu^I(NH_3)_2]^+$-O_2-$[Cu^I(NH_3)_2]^+$ intermediate is highly dependent on Cu loadings. For the mobile $[Cu^I(NH_3)_2]^+$ intermediate, considering the facts that (1) Cu^I and N both have atomic sizes > 0.5 Å, and (2) the Cu-N bond length is ~2 Å and the N-H bond length is ~1 Å, transporting through Chabazite pores (~3.8 Å) will be sterically hindered unless it adopts the right orientation relative to the pore opening. Since random orientation of $[Cu^I(NH_3)_2]^+$ relative to pore openings is expected, it is very understandable that at low Cu loadings, $[Cu^I(NH_3)_2]^+$ transport can be a slow, i.e., rate limiting, process.

In order to verify that diffusion limitation can indeed control the transport of $[Cu^I(NH_3)_2]^+$ at low Cu loadings, the diffusion coefficient for $[Cu^I(NH_3)_2]^+$ in Cu/SZZ-13 was calculated using an *ab initio* molecular dynamics (AIMD) simulation method. The AIMD simulation was performed in the canonical (NVT) ensemble with Nose-Hoover thermostat[24] set to 200 °C. The time step was 0.5 fs and the total AIMD simulation time was 10 ps. As shown in Figure S5, the slope of the root mean square deviation (RMSD) with respect to time is the diffusion coefficient D, where D = RMSD/6t = 4.4×10^{-12} (m^2/s). Note that this value falls well within the intracrystalline diffusion regime (< ~10^{-8} m^2/s).[25] Even though the small D value itself does not prove that low-temperature SCR must be diffusion limited by $[Cu^I(NH_3)_2]^+$ transport, its bulky nature and electrostatic attractions with the zeolite framework make this highly likely at low $[Cu^I(NH_3)_2]^+$ concentrations. More importantly, our kinetics results collected at low Cu loadings are only consistent with the presence of such a rate limiting factor.

As described above, Janssens et al. recently proposed an oxidation half-cycle pathway for the direct oxidation of individual Cu(I) to Cu(II) by O_2+NO via formation of a nitrate intermediate.[8] Herein DFT was also used to calculate another possible pathway; that is, oxidation of *individual* $[Cu^I(NH_3)_2]^+$ by O_2+NO in the presence of H^+ to regenerate the $[(NH_3)_2$-Cu^{II}-$OH]^+$ active site. The detailed reaction profile is displayed in Figure S6. The activation barrier for this pathway is as high as 175 kJ/mol, highly unlikely at low reaction temperatures. Again, this corroborates our argument that reoxidation of individual Cu(I) to Cu(II) by O_2+NO should only be considered as a high-temperature process.

It is worthwhile noting that there has been, thus far, no spectroscopic evidence for the formation of a transient dimeric Cu intermediate. For example, the recent study by Lomachenko et al. stated clearly that FT-EXAFS do not show any signal ascribable to Cu-Cu scattering paths.[11] However, this should not be taken as solid evidence against our proposed mechanism. In particular, as stated in the classic Thomas & Thomas text book, *the transitory nature of some of the intermediates implicated in catalysis are such that their structures can best be ascertained by computational procedures, rather than by direct, experimental ones*.[26] The low-temperature standard NH_3-SCR mechanism proposed in the present study is the only one that is fully consistent with low-temperature SCR kinetics, and is demonstrated here to be energetically feasible from theoretical calculations. We argue here that proposals only involving redox of individual isolated Cu-ions are incomplete. Finally, this study shows that the catalytic standard NH_3-SCR process naturally links homo- and heterogeneous catalysis, demonstrating the importance of the reaction media on the dynamics of the active sites and reaction kinetics.

CONCLUSION

Under well controlled differential reaction condition, standard SCR over low Cu-loaded Cu/SSZ-13 displays complex temperature and Cu loading dependence. At low temperatures (<250 °C), SCR rates depend linearly on square of Cu loading while at high temperatures (>350 °C), SCR rates depend linearly on Cu loading. With the aid from DFT calculations, we demonstrate that the low-temperature oxidation half-cycle of the SCR reaction cannot be achieved on isolated Cu-ions; O_2 activation requires participation of a pair of mobile $[Cu^I(NH_3)_2]^+$ sites with the formation of a $[Cu^I(NH_3)_2]^+$-O_2-$[Cu^I(NH_3)_2]^+$ intermediate. This chemistry occurs homogeneously within the SSZ-13 pores and is the rate-limiting step at low Cu loadings. At high temperatures, isolated Cu-ions anchor on the SSZ-13 framework and become immobilized. In this case, the oxidation half-cycle occurs on isolated Cu(I) sites with rather high activation barriers.

EXPERIMENTAL SECTION

Sample preparation. SSZ-13 materials were synthesized hydrothermally in house. The synthesis for SSZ-13 with Si/Al = 6 via a static hydrothermal method has been described in detail elsewhere.[27, 28] The SSZ-13 with Si/Al = 12 was synthesized under continuous gel stirring, which has also been described in detail elsewhere.[29] Cu/SSZ-13 samples were prepared using a standard two-step solution ion exchange protocol reported previously, first with NH_4NO_3 followed by $CuSO_4$ solutions at 80 °C.[4, 5] In particular, to prepare Cu/SSZ-13 with exceedingly low Cu loadings, dilute $CuSO_4$ solutions at 0.001 M were used. The as-synthesized Cu/SSZ-13 catalysts were dried and then calcined in static air at 550 °C for 5-8 hours before use. Structural integrity of the catalysts was routinely monitored with XRD and surface area/pore volume analyses. Si, Al and Cu contents were determined with Inductively Coupled Plasma Atomic Emission Spectroscopy (ICP-AES) at Galbraith Laboratories (Knoxville, TN, USA). Cu contents were further confirmed from Electron Paramagnetic Resonance (EPR) analysis.[4]

Reaction tests. Standard NH_3-SCR ($4NH_3 + 4NO + O_2 = 4N_2 + 6H_2O$) reaction kinetics measurements were carried out in a plug-flow reaction system described elsewhere.[4, 5] Powder samples were pressed, crushed and sieved (0.18-0.25 mm) prior to use. The feed gas contained 350 ppm NO, 350 ppm NH_3, 14% O_2, 2.5% H_2O and balance N_2. All of the gas lines were heated to over 100 ºC to avoid water condensation. Concentrations of reactants and products were measured by an online Nicolet Magna 560 FTIR spectrometer with a 2 m gas cell maintained at 150 ºC. Prior to temperature-dependent steady-state reaction measurements, the catalysts were activated in 14% O_2/N_2 flow for 1 h at 550 ºC. At each target temperature, a minimum waiting time of ~45 min was applied to reach a steady-state. Typically, the total gas flow was 300 sccm, and the gas hourly space velocity (GHSV) was estimated to be ~400,000 h^{-1} for a catalyst amount of 30 mg. For reactions carried out at ~350 ºC and above, a much higher GHSV of ~1,200,000 h^{-1} was chosen to maintain differential conversions. Reaction data were routinely checked to verify whether these are kinetically benign using the Koros-Nowak criterion.[5, 6] NO_x and NH_3 conversions were calculated based on the following equations:

$$NO_x\ Conversion\ \% = \frac{(NO+NO_2)_{inlet} - (NO+NO_2+N_2O)_{outlet}}{(NO+NO_2)_{inlet}} \times 100$$

$$NH_3\ Conversion\ \% = \frac{(NH_3)_{inlet} - (NH_3)_{outlet}}{(NH_3)_{inlet}} \times 100$$

Computational methods. Periodic DFT calculations were performed using the CP2K code.[30] All DFT calculations employed a mixed Gaussian and planewave basis sets. Core electrons were represented with norm-conserving Goedecker-Teter-Hutter pseudopotentials,[31-33] and the valence electron wavefunction was expanded in a double-zeta basis set with polarization functions[34] along with an auxiliary plane wave basis set with an energy cutoff of 360 eV. Larger cutoff energies of 500 and 600 eV with PBE functional, as well as HSE06 functional were also tested to confirm the accuracy of the calculation results (Table S1). The generalized gradient approximation exchange-correlation functional of Perdew, Burke, and Enzerhof (PBE)[35] was used. The adsorption and reaction intermediate configurations were optimized with the Broyden-Fletcher-Goldfarb-Shanno (BGFS) algorithm with SCF convergence criteria of 1.0×10^{-8} au. It was found that the calculated total energy difference was negligible (<0.01 eV) when the maximum force convergence criteria of 0.001 hartree/bohr was used. To compensate the long-range van der Waals dispersion interaction between the adsorbate and the zeolite framework, the DFT-D3 scheme[36] with an empirical damped potential term was added into the energies obtained from exchange-correlation functional in all calculations. The vibrational frequencies of the molecules of interest were calculated in the harmonic oscillator approximation with a displacement of 0.01 Å. Only the mobile reactants and neighboring water molecules were considered while the atoms on the zeolite frame treated as fixed. The SSZ-13 zeolite structure was modelled using two hexagonal unit cells (totally 72 T atoms) with the size parameters of 13.6750×23.6858×14.7670 Å^3. To mimic technically relevant Cu/SSZ-13 catalysts with Si/Al ratios of ~12-18, 6 Si atoms within the SSZ-13 model structure were replaced by 6 Al atoms, obtaining a model structure with the Si/Al ratio of 11. 6 H atoms were also introduced on the O_1 position of four O atoms connected with the Al atom to keep the structure charge neutral.[37] On the basis of previous theoretical studies[7-9, 21] and considerations shown above, $[Cu^{II}(OH)]^+$ located in the window of eight membered ring was optimized as the initial configuration of the active center. More details regarding the computation can be found in the supporting information.

ASSOCIATED CONTENT

Supporting Information. Details on the DFT calculations, including optimized structure of Cu/SSZ-13 with 72 T atoms, DFT calculated reaction profiles for the reduction half-cycle pathways, DFT calculated reaction profile for the formation of $[Cu^{II}(NH_3)_2]^{2+}$-O-$[Cu^{II}(NH_3)_2]^{2+}$ intermediate, DFT calculated hydrolysis reaction profile for the formation of the initial active site $[(NH_3)_2$-Cu^{II}-$OH]^+$, *ab initio* molecular dynamics (AIMD) simulation of the diffusion of $[Cu^{I}(NH_3)_2]^+$ in Cu/SSZ-13, and DFT calculated reaction profile for the direct oxidation of single isolated Cu(I) to Cu(II) by O_2 and NO, as well as calculated Gibbs free energies (kJ/mol) for the oxidation half-cycle with the participation of two $[Cu^{I}(NH_3)_2]^+$ intermediates using different functionals and cutoff energies, have been supplied as Supporting Information. This material is available free of charge via the Internet at http://pubs.acs.org.

AUTHOR INFORMATION

Corresponding Author

* F. Gao (feng.gao@pnnl.gov) and D. Mei (donghai.mei@pnnl.gov) are the authors to whom correspondence should be addressed.

ACKNOWLEDGMENT

The authors gratefully acknowledge the US Department of Energy (DOE), Energy Efficiency and Renewable Energy, Vehicle Technologies Office for the support of this work. The research described in this paper was performed in the Environmental Molecular Sciences Laboratory (EMSL), a national scientific user facility sponsored by the DOE's Office of Biological and Environmental Research and located at Pacific Northwest National Laboratory (PNNL). PNNL is operated for the US DOE by Battelle.

REFERENCES

1. Beale, A. M.; Gao, F.; Lezcano-Gonzalez, I.; Peden, C. H. F.; Szanyi, J. *Chem Soc Rev* **2015,** 44, 7371-7405.
2. Gao, F.; Kwak, J. H.; Szanyi, J.; Peden, C. H. F. *Top Catal* **2013,** 56, 1441-1459.
3. Deka, U.; Lezcano-Gonzalez, I.; Weckhuysen, B. M.; Beale, A. M. *Acs Catal* **2013,** 3, 413-427.
4. Gao, F.; Walter, E. D.; Karp, E. M.; Luo, J. Y.; Tonkyn, R. G.; Kwak, J. H.; Szanyi, J.; Peden, C. H. F. *J Catal* **2013,** 300, 20-29.
5. Gao, F.; Walter, E. D.; Kollar, M.; Wang, Y. L.; Szanyi, J.; Peden, C. H. F. *J Catal* **2014,** 319, 1-14.
6. Bates, S. A.; Verma, A. A.; Paolucci, C.; Parekh, A. A.; Anggara, T.; Yezerets, A.; Schneider, W. F.; Miller, J. T.; Delgass, W. N.; Ribeiro, F. H. *J Catal* **2014,** 312, 87-97.
7. Paolucci, C.; Verma, A. A.; Bates, S. A.; Kispersky, V. F.; Miller, J. T.; Gounder, R.; Delgass, W. N.; Ribeiro, F. H.; Schneider, W. F. *Angew Chem Int Edit* **2014,** 53, 11828-11833.
8. Janssens, T. V. W.; Falsig, H.; Lundegaard, L. F.; Vennestrom, P. N. R.; Rasmussen, S. B.; Moses, P. G.; Giordanino, F.; Borfecchia, E.; Lomachenko, K. A.; Lamberti, C.; Bordiga, S.; Godiksen, A.; Mossin, S.; Beato, P. *Acs Catal* **2015,** 5, 2832-2845.
9. Paolucci, C.; Parekh, A. A.; Khurana, I.; Di Iorio, J. R.; Li, H.; Caballero, J. D. A.; Shih, A. J.; Anggara, T.; Delgass, W. N.; Miller, J. T.; Ribeiro, F. H.; Gounder, R.; Schneider, W. F. *J Am Chem Soc* **2016,** 138, 6028-6048.
10. McEwen, J. S.; Anggara, T.; Schneider, W. F.; Kispersky, V. F.; Miller, J. T.; Delgass, W. N.; Ribeiro, F. H. *Catal Today* **2012,** 184, 129-144.
11. Lomachenko, K. A.; Borfecchia, E.; Negri, C.; Berlier, G.; Lamberti, C.; Beato, P.; Falsig, H.; Bordiga, S. *J Am Chem Soc* **2016,** 138, 12025–12028.
12. Kwak, J. H.; Zhu, H. Y.; Lee, J. H.; Peden, C. H. F.; Szanyi, J. *Chem Commun* **2012,** 48, 4758-4760.
13. Kwak, J. H.; Varga, T.; Peden, C. H. F.; Gao, F.; Hanson, J. C.; Szanyi, J. *J Catal* **2014,** 314, 83-93.
14. Clemens, A. K. S.; Shishkin, A.; Carlsson, P. A.; Skoglundh, M.; Martinez-Casado, F. J.; Matej, Z.; Balmes, O.; Harelind, H. *Acs Catal* **2015,** 5, 6209-6218.
15. Giordanino, F.; Borfecchia, E.; Lomachenko, K. A.; Lazzarini, A.; Agostini, G.; Gallo, E.; Soldatov, A. V.; Beato, P.; Bordiga, S.; Lamberti, C. *J Phys Chem Lett* **2014,** 5, 1552-1559.
16. Long, R. Q.; Yang, R. T. *J Catal* **2002,** 207, 274-285.
17. Kwak, J. H.; Lee, J. H.; Burton, S. D.; Lipton, A. S.; Peden, C. H. F.; Szanyi, J. *Angew Chem Int Edit* **2013,** 52, 9985-9989.
18. Vannice, M. A., *Kinetics of Catalytic Reactions*. Springer ScienceþBusiness Media, Inc.: New York, 2005.
19. Gao, F.; Wang, Y. L.; Washton, N. M.; Kollar, M.; Szanyi, J.; Peden, C. H. F. *Acs Catal* **2015,** 5, 6780-6791.
20. Broach, R. W., Zeolite Types and Structures. In *Zeolites in Industrial Separation and Catalysis*, Kulprathipanja, S., Ed. 2010 WILEY-VCH Verlag GmbH & Co. KGaA: Weinheim, 2010; pp 27-59.
21. Zhang, R. Q.; McEwen, J. S.; Kollar, M.; Gao, F.; Wang, Y. L.; Szanyi, J.; Peden, C. H. F. *Acs Catal* **2014,** 4, 4093-4105.
22. Centi, G.; Perathoner, S. *Appl Catal a-Gen* **1995,** 132, 179-259.
23. Brandenberger, S.; Krocher, O.; Tissler, A.; Althoff, R. *Catal Rev* **2008,** 50, 492-531.
24. Nosé, S. *J. Chem. Phys.* **1984,** 81, 511-519.
25. Ruthven, D. M., Diffusion in Zeolite Molecular Sieves. In *Introduction to Zeolite Science and Practice - 3rd Revised Edition*, Cejka, J.; Van Bekkum, H.; Corma, A.; Schuth, F., Eds. Elsevier B. V. : 2007; pp 737-785; Amsterdam, Netherlands.
26. Thomas, J. M.; Thomas, W. J., *Principles and practics of heterogeneous catalysis*. VCH: Weinheim; New York; Basel; Cambridge; Tokyo, 1996.
27. Fickel, D. W.; Lobo, R. F. *J Phys Chem C* **2010,** 114, 1633-1640.
28. Fickel, D. W.; D'Addio, E.; Lauterbach, J. A.; Lobo, R. F. *Appl Catal B-Environ* **2011,** 102, 441-448.
29. Gao, F.; Washton, N. M.; Wang, Y. L.; Kollár, M.; Szanyi, J.; Peden, C. H. F. *J Catal* **2015,** 331, 25-38.
30. VandeVondele, J.; Krack, M.; Mohamed, F.; Parrinello, M.; Chassaing, T.; Hutter, J. *Comput. Phys. Commun.* **2005,** 167, 103-128.
31. Goedecker, S.; Teter, M.; Hutter, J. *Phys. Rev. B* **1996,** 54, 1703-1710.
32. Hartwigsen, C.; Goedecker, S.; Hutter, J. *Phys. Rev. B* **1998,** 58, 3641-3662.
33. Krack, M.; Parrinello, M. *Phys. Chem. Chem. Phys.* **2000,** 2, 2105-2112.
34. VandeVondele, J.; Hutter, J. *J. Chem. Phys.* **2007,** 127, 114105.
35. Perdew, J. P.; Burke, K.; Ernzerhof, M. *Phys. Rev. Lett.* **1996,** 77, 3865.
36. Grimme, S.; Antony, J.; Ehrlich, S.; Krieg, H. *J. Chem. Phys.* **2010,** 132, 154104.
37. Nielsen, M.; Brogaard, R. Y.; Falsig, H.; Beato, P.; Swang, O.; Svelle, S. *ACS Catal.* **2015,** 5, 7131-7139.

TOC